ORIGINAL ARTICLE

Correlating ROS1 Protein Expression With *ROS1* Fusions, Amplifications, and Mutations

Richard S. P. Huang, MD,[a,*] Amanda Gottberg-Williams, BS,[a] Panhia Vang, BS,[a] Shoua Yang, HSD,[a] Nicholas Britt, BS,[a] Jaspreet Kaur, MS,[b] James Haberberger, BS,[a] Natalie Danziger, BS,[b] Clarence Owens, BS,[a] Sara E. Beckloff, PhD,[a] Jeffrey S. Ross, MD,[b,c] Shakti H. Ramkissoon, MD, PhD[a,d]

[a]*Foundation Medicine, Inc., Morrisville, North Carolina*
[b]*Foundation Medicine, Inc., Cambridge, Massachusetts*
[c]*Department of Pathology, State University of New York (SUNY) Upstate Medical University, Syracuse, New York*
[d]*Department of Pathology, Wake Forest School of Medicine, Winston-Salem, North Carolina*

Received 11 September 2020; accepted 11 September 2020
Available online - 18 September 2020

ABSTRACT

Introduction: In this study, we sought to further characterize ROS1 protein expression in solid tumors with the complete spectrum of *ROS1* genomic alterations.

Methods: ROS1 immunohistochemistry (IHC) was performed using the ROS1 (SP384) class I assay per manufacturer's instructions on a variety of solid tumors (n = 32) with known *ROS1* genomic alterations. Genomic alterations included fusions (n = 17), gene amplifications (n = 10), and short-variant mutations (n = 11).

Results: Of the 32 cases with ROS1 IHC results, 100% (11 of 11) with canonical *ROS1* fusions were positive for ROS1 IHC. Among noncanonical *ROS1* fusions, only two (of five) cases with *SQSTM1-ROS1* and *RDX-ROS1* fusions were positive for ROS1 IHC whereas *PTPRK-ROS1* (two) and *TTC28-ROS1* fusions were negative for ROS1 IHC. One sample with a canonical *ROS1* fusion and co-occurring *ROS1* resistance mutation (6094G>A, p.G2032R) was positive for ROS1 IHC. A total of 10% (one of 10) of *ROS1* amplified tumors were positive for ROS1 IHC. None of the cases (zero of five) with *ROS1* short-variant mutations were positive for ROS1 protein expression.

Conclusions: These findings suggest that if ROS1 IHC was used as a screening tool for *ROS1* fusion, a subset of fusion-negative tumors will reveal positive IHC staining highlighting the value of reflexing to genomic profiling to confirm the presence of a targetable fusion-driver before the initiation of therapy. In addition, the ability of comprehensive genomic profiling to detect *ROS1* resistance mutations will be important for clinical decision making.

Keywords: ROS1; Protein expression; Fusions; Amplifications; Mutations

Introduction

ROS1 is a proto-oncogene located on chromosome 6p22.1 that encodes a receptor tyrosine kinase.[1] Typically, malignant tumors with *ROS1* fusions overexpress oncogenic ROS1 protein on the tumor cells.[2-4] Importantly, ROS1 tyrosine kinase inhibitor (TKI) has been reported to be highly efficacious in patients with NSCLC harboring *ROS1* rearrangements that activate the kinase domain of the ROS1 protein.[4]

Two ROS1 TKIs, crizotinib and entrectinib, have been approved by the U.S. Food and Drug Administration as a

*Corresponding author.

Disclosure: All authors are employees of Foundation Medicine and receive a salary and/or stock equity from Foundation Medicine.

Address for correspondence: Richard S.P. Huang, MD, Foundation Medicine, Inc., 7010 Kit Creek Road, Morrisville, NC 27560. E-mail: rhuang@foundationmedicine.com

Cite this article as: Huang RSP, et al. Correlating ROS1 Protein Expression With *ROS1* Fusions, Amplifications, and Mutations. JTO Clin Res Rep 2:100100

ISSN: 2666-3643

https://doi.org/10.1016/j.jtocrr.2020.100100

therapy for *ROS1*-positive NSCLC.[5,6] In the clinical trials that enabled the approvals of these ROS1 TKIs, multiple diagnostic assay methodologies were used to determine *ROS1* status including DNA-based or RNA-based next-generation sequencing (NGS), fluorescence in situ hybridization (FISH), or polymerase chain reaction.[7,8] In the PROFILE 1001 clinical trial that enabled the approval of crizotinib in *ROS1* rearrangement tumors, five known and two novel partner genes were identified by these assays and the specific type of rearrangement did not reveal differences in clinical response to crizotinib. Though not used as the diagnostic method to detect ROS1 positivity in the aforementioned clinical trials, in the current National Comprehensive Cancer Network and the College of American Pathologists/Association of Molecular Pathology/the International Association for the Study of Lung Cancer testing guidelines, ROS immunohistochemistry (IHC) is deemed sufficient as a screening tool.[9,10] However, it is recommended that a positive result by ROS1 IHC be followed up with a molecular or cytogenetic method.

Currently, the only commercially available class I ROS1 IHC assay is the ROS1 SP384 IHC assay; however, a less sensitive D4D5 antibody is available as a research use only assay.[11,12] Nong et al.[13] compared the detection of *ROS1* fusions using NGS and the D4D5 antibody. The conclusion of the study was that NGS could exclude false positivity of *ROS1* fusions detected by IHC. It is important to point out that this study used D4D5 antibody and not the SP384 antibody and used an IHC staining protocol and a scoring system that has not been standardized or validated with a large cohort of patients. To the best of our knowledge, there are only two large cohorts in the literature that compared the ROS1 (SP384) assay with *ROS1* genomic alterations.[11,12,14] In the first study by Huang et al.,[14] the ROS1 SP384 was compared with ROS1 FISH detected rearrangement status with high sensitivity and specificity (100%, 98%, respectively) with the 2+ (or above) cytoplasmic staining in more than 30% of total tumor cells cut-off.[14] Although there was a small subset of patients with concurrent NGS and polymerase chain reaction testing in that study, most of the patients were evaluated only by FISH testing, and so the fusion partner for most of the cases was unknown. Similarly, in the ROSING study, FISH rearrangement was the main comparator, although for a subset of patients, NGS was performed (fusion partners identified: *CD74*, *EZR*, *SDC4*, *SLC34A2*, and *TPM3*).[11] Although studies have already established the sensitivity and specificity of SP384 in detecting canonical *ROS1* fusions, examination of ROS1 SP384 in the detection of *ROS1* noncanonical fusions, *ROS1* amplifications, and *ROS1* mutations is lacking in the literature.

Because of the increased clinical adoption of high throughput technologies, such as comprehensive genomic profiling (CGP), an increasing number of *ROS1* fusion partners have been identified (33 *ROS1* fusion partners to date).[15–22] Although the higher prevalence *ROS1* fusions partners, such as *CD74*, *EZR*, *SDC4*, *SLC34A2*, and *TPM3* (canonical), have been widely studied, ROS1 oncogenic protein expression in some of these rare fusion partners (noncanonical) has not been studied and their response to ROS1 TKIs is unclear. In addition, questions remain whether amplifications in the *ROS1* gene can potentially result in an overexpression of ROS1 protein and thus generate a possible therapeutic target to ROS1 TKIs. Also, although acquired *ROS1* mutations in tumors exposed to anti-ROS1 targeted therapies have been reported to result in resistance of ROS1 TKIs, their effect on ROS1 protein expression has not been well characterized.[23,24] In this study, using a large genomics database, we sought to compare and contrast ROS1 protein expression status in solid tumor cases across the complete spectrum of *ROS1* genomic alterations.

Materials and Methods

Patient Cohort

Approval for this study was obtained from the Western Institutional Review Board protocol no. 20152817 with an appropriate waiver of consent. Patient demographic information and specimen site were extracted from accompanying pathology reports (Table 1). A retrospective analysis of our clinicogenomic database identified 32 cases with *ROS1* genomic alterations, including 11 canonical fusion, five noncanonical fusions, 10 amplifications, five short-variant mutations, and one canonical fusion with a co-occurring *ROS1* resistance mutation. For all cases, *ROS1* genomic alterations were detected by CGP using the hybrid capture-based FoundationOne or FoundationOneCDx assay.

DNA Sequencing Assay

FoundationOne and FoundationOneCDx are CGP assays that are performed in a laboratory certified by the Clinical Laboratory Improvement Amendments and accredited by the College of American Pathologists (Foundation Medicine, Cambridge, MA). FoundationOne and FoundationOneCDx uses a hybrid capture methodology and detects base substitutions, insertions, deletions, and copy number (CN) alterations in up to 324 genes and select gene rearrangements in up to 36 genes, and tumor mutation burden and microsatellite instability using the previously described methods.[25] All *ROS1* exons and introns 31 to 35 were baited for in FoundationOne and FoundationOneCDx. An

Table 1. Patient and Sample Characteristics of Tumors With *ROS1* Genomic Alterations

Patient Characteristic	Metric
Median age (y)	60.5
Mean age (y)	60.7
Sex (female:male)	0.71875
Predominant ancestry	
African	6.3% (2/32)
Central and South American	15.6% (5/32)
East Asian	6.3% (2/32)
European	68.8% (22/32)
South Asian	3.1% (1/32)
Primary site	
Lung	53.1% (17/32)
Breast	15.6% (5/32)
Unknown	12.5% (4/32)
Ovary	9.4% (3/32)
Ampulla	3.1% (1/32)
Skin	3.1% (1/32)
Colon	3.1% (1/32)
Metastatic specimens[a]	50% (14/28)
Site of metastasis	
Lymph node	35.7% (5/14)
Lung	21.4% (3/14)
Liver	14.3% (2/14)
Pelvis	7.1% (1/14)
Pleural cavity	7.1% (1/14)
Brain	7.1% (1/14)
Omentum	7.1% (1/14)

[a]Four cases are CUP.
CUP, carcinoma of unknown primary.

anatomical pathology board-certified pathologist reviewed each sample's hematoxylin and eosin–stained slide under light microscopy to determine the suitability for FoundationOne and FoundationOneCDx testing by examining for at least 20% tumor nuclei present and to determine the diagnosis of the sample (the accompanying pathology report is also used to help determine diagnosis). Predominant genetic ancestry was assessed using a single nucleotide polymorphism–based approach as previously described.[26,27]

ROS1 (SP384) Class I Assay

ROS1 (SP384) testing was performed using the ROS1 (SP384) class 1 assay per manufacturer's instructions.[28] Briefly, ROS1 (SP384) class I assay (Ventana Medical Systems Inc., Tucson, AZ) is an IHC assay that consists of the ROS1 (SP384) antibody with the OptiView DAB IHC Detection Kit (Ventana Medical Systems Inc.) stained on a Benchmark Instrument (Ventana Medical Systems Inc.) using the recommended staining protocol for ROS1 (SP384). As recommended by the manufacturer, a rabbit monoclonal negative control was used as a negative reagent control and reactive type II alveolar pneumocytes from normal lung was used as the positive system–level run control.

Pathologist Evaluation of ROS1 IHC

All controls were determined to be adequate before interpretation of the ROS1 IHC cases. All stained IHC slides were interpreted by a single board-certified pathologist (R.S.P.H.) (American Board of Pathology). The percentage of tumor cell cytoplasmic staining intensity (ranged from an intensity of 0, 1+, 2+, and 3+) was evaluated for each case. Staining intensity was defined as absence of staining (0), weak staining (1+), moderate staining (2+), and strong staining (3+). For the purposes of this study, we used staining in the cytoplasm of 2+ (or above) in greater than 30% of total tumor cells as being considered positive for ROS1 IHC, similar to the study that compared the ROS1 SP384 assay with FISH testing by Huang et al.[14] In addition, we also explored whether a case had any expression of ROS1 protein defined as 1+ (or above) staining in the cytoplasm of more than 1% of total tumor cells.

Results

Patient Characteristics

The median age of our cohort was 60.5 years, mean age was 60.7 years, and female-to-male ratio was 17:15. Predominant genetic ancestry was European (68.8%, 22

Table 2. Percentage Staining of Tumor Cells in Solid Tumors With a Variety of *ROS1* Genomic Alterations

Patient ID	*ROS1* Alterations	Diagnosis[a]	% 0%	% 1+	% 2+	% 3+	IHC Status
	Common fusions						
1	*CD74*(ex1-6)-*ROS1*(ex34-43)	Lung adenoCA[b]	0	0	10	90	POS
2	*CD74*(ex1-6)-*ROS1*(ex34-43)	Lung adenoCA[b]	0	0	10	90	POS
3	*CD74*(ex1-6)-*ROS1*(ex33-43)	Lung adenoCA (mucinous lepidic)	0	0	30	70	POS
4	*CD74*(ex1-6)-*ROS1*(ex34-43)	Lung adenoCA (solid)	0	0	0	100	POS
5	*CD74*(ex1-6)-*ROS1*(ex33-43)	Lung adenoCA (solid)	0	0	10	90	POS
6[c]	*EZR*(ex1-9)-*ROS1*(ex33-43)	Lung adenoCA (solid)	0	0	10	90	POS
7	*EZR*(ex1-9)-*ROS1*(ex34-43)	Lung adenoCA (mucinous lepidic)	20	30	40	10	POS
8	*EZR*(ex1-9)-*ROS1*(ex34-43)	Lung adenoCA[b]	0	0	50	50	POS
9[c]	*EZR*(ex1-9)-*ROS1*(ex33-43)	Lung adenoCA (acinar)	0	10	90	0	POS
10	*SDC4*(ex1-2)-*ROS1*(ex32-43)	Lung adenoCA (mucinous lepidic)	5	15	40	40	POS
11	*SLC34A2*(ex1-13)-*ROS1*(ex32-43)	Lung adenoCA (solid)	0	0	10	90	POS
	Uncommon fusions						
12	*PTPRK*(ex1-15)-*ROS1*(ex33-43)	Unknown primary CA	99	1	0	0	NEG
13	*PTPRK*(ex1-2)-*ROS1*(ex35-43)	Breast-invasive ductal CA	100	0	0	0	NEG
14	*TTC28*(ex1-1)-*ROS1*(ex35-43)	Colon adenoCA	100	0	0	0	NEG
15	*SQSTM1*(ex1-2)-*ROS1*(ex34-43)	Lung adenoCA (solid)	0	0	50	50	POS
16	*RDX*(ex1-10)-*ROS1*(ex34-43)	Unknown primary adenoCA	20	20	30	30	POS
	Fusion + mutation						
17	*SDC4*(ex1-5)-*ROS1*(ex34-43); 6094G>A (p.G2032R)	Lung adenoCA (solid)	0	0	25	75	POS
	Amplification						
18	CN: 7	Lung squamous cell CA	85	10	5	0	NEG
19	CN: 18	Breast CA	100	0	0	0	NEG
20	CN: 9	Lung adenoCA[b]	100	0	0	0	NEG
21	CN: 22	Ovary serous CA	100	0	0	0	NEG
22	CN: 8	Breast CA	100	0	0	0	NEG
23	CN: 20	Ampullary adenoCA	100	0	0	0	NEG
24	CN: 7	Breast CA	100	0	0	0	NEG
25	CN: 9	Ovary serous CA	100	0	0	0	NEG
26	CN: 10	Lung adenoCA (solid)	0	0	20	80	POS
27	CN: 9	Breast CA	100	0	0	0	NEG
	Mutations						
28	6551G>T (p.R2184I)	Ovary CA mixed histology	100	0	0	0	NEG
29	4652G>A (p.G1551E/), 4902+1G>A (p.splice site 4902+1G>A), 3362_3363GA>AT (p.R1121N)	Unknown primary CA	100	0	0	0	NEG
30	4924G>A (p.E1642K), 4652G>A (p.G1551E), 2651C>T (p.S884F), 205C>T (p,Q69[c])	Skin melanoma	100	0	0	0	NEG
31	949C>T (p.R317W)	Unknown primary neuroendocrine CA	100	0	0	0	NEG
32	2548C>G (p.Q850E)	Lung squamous cell CA	100	0	0	0	NEG

[a]CA; predominant lung adenocarcinoma histologic pattern in parenthesis, when available.
[b]Cytology specimen: lung adenocarcinoma histologic pattern not available.
[c]Membranous staining in 80% of tumor cells.
CA, carcinoma; CN, copy number; ID, identification document; IHC, immunohistochemistry; NEG, negative; POS, positive.

of 32), and half (50%, 14 of 28) of the specimens were from a metastatic site (Table 1).

Genomic Landscape of ROS1 Alterations

The study cohort consisted of 32 *ROS1* altered samples, including 11 cases (34.4%) with a canonical fusion partner (*CD74*, *EZR*, *SDC4*, and *SLC34A1*), five cases (15.6%) with a noncanonical fusion partner (*PTPRK*x2, *TTC28*, *SQSTM1*, and *RDX*), one case (3.1%) with a *SDC4-ROS1* fusion and co-occurring *ROS1* resistance mutation (6094 G>A [p.G2032R]), 10 cases (31.3%) with *ROS1* amplification, and five cases (15.6%) with *ROS1* mutations (Table 2). The *ROS1* tyrosine kinase domain (exons 36–42) was preserved in all the canonical and noncanonical *ROS1* fusions. All canonical *ROS1* fusions

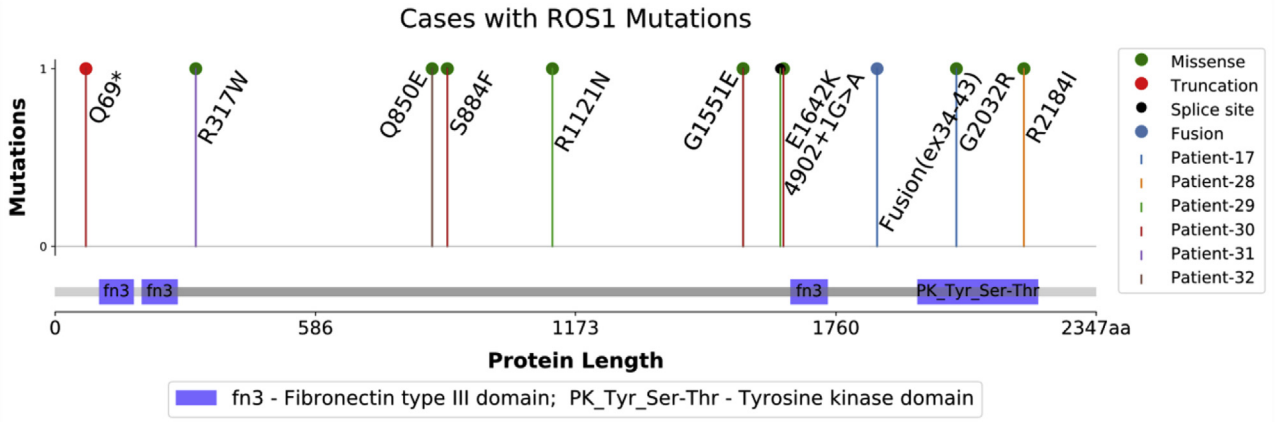

Figure 1. Lollipop plot of the locations of the *ROS1* mutations on the *ROS1* gene. A variety of *ROS1* mutations were present, including one truncation mutation, one splice site mutation, and multiple missense mutations. Two mutations are in the *ROS1* tyrosine kinase domain. Patient 17 had both a *ROS1* fusion and a *ROS1* known resistance mutation, and patient 29 and patient 30 each had multiple *ROS1* mutations. *Patient 29 also had a G1551E mutation that is not revealed on the plot.

were identified in lung adenocarcinomas, whereas noncanonical fusions were detected in lung adenocarcinoma, breast-invasive ductal carcinoma, unknown primary carcinoma, and colon adenocarcinoma.

ROS1 amplifications ranged from a CN of seven to 22 with a mean CN of 12 and median CN of nine. Like the noncanonical fusions, *ROS1* amplification cases were composed of a wide variety of tumor types (Table 2). A variety of *ROS1* short-variant mutations were evaluated, including one truncation mutation, one splice site mutation, and multiple missense mutations. Two mutations were in the *ROS1* tyrosine kinase domain (Fig. 1). Patient 17 had both a *ROS1* fusion and a *ROS1* known resistance mutation, and patient 29 and patient 30 each had multiple *ROS1* mutations (Fig. 1).

Correlation of ROS1 Genomic Alterations With ROS1 IHC Results

All canonical *ROS1* fusions exhibited ROS1 IHC positivity (11 of 11), whereas only 40% (two of five) of the cases with noncanonical *ROS1* fusions exhibited IHC positivity. The one case with a common *ROS1* fusion and co-occurring *ROS1* resistance mutation was considered positive for ROS1 IHC; of the 10 *ROS1* amplified cases, one case (10%) was considered positive for ROS1 IHC. None of the cases with *ROS1* mutations were positive for ROS1 IHC or exhibited any ROS1 protein expression. Representative images of all 32 cases are provided as a supplemental image atlas (Supplementary Figs. 1–3).

We also examined the presence of ROS1 expression defined as 1+ (or above) staining intensity in the cytoplasm of more than 1% of total tumor cells. Using this definition for ROS1 expression, the results were very similar to the ROS1 IHC positivity definition. The only difference here is that 60% (three of five) of the noncanonical fusions and 20% (two of 10) of the amplifications had ROS1 protein expression. Specifically, patient 12 (*PTPRK-ROS1*) had 1% of cytoplasmic tumor cells staining at 1+ (weak intensity) and was negative for ROS1 IHC because it did not meet the established scoring threshold. In addition, patient 18 (CN7) with 10% of tumor cells at 1+ (weak intensity) cytoplasmic staining and 5% of tumor cells at 2+ (moderate intensity) cytoplasmic staining was also considered negative for ROS1 IHC.

Overall, ROS1 IHC staining in this cohort exhibited little heterogeneity and no difficulty was encountered when determining the ROS1 IHC status of the cases in the cohort (Fig. 2). No cases had nuclear staining in the tumor cells, and two cases had membranous staining in addition to the cytoplasmic staining present (patients 6 and 9, both with *EZR-ROS1* fusions). Other important staining patterns and artifacts were observed in the review of the ROS1 IHC–stained slides (Fig. 3). For example, we saw moderate-to-strong staining in some reactive type II pneumocytes, light brown staining of hemosiderin, and yellow-brown staining of melanin pigment.

Discussion

In our study, consistent with the literature, all the canonical fusion partners (*CD74*, *EZR*, *SDC4*, and *SLC34A2*) stained quite strongly by the ROS1 SP384 assay and were considered positive on the basis of the aforementioned cutoff. In the five cases of noncanonical fusions as detected by NGS in our cohort, two (fusion partners *RDX* and *SQSTM1*) also stained strongly and were considered positive in our analysis. These findings suggest that these fusion genes activated the ROS1 kinase domain, resulting in an oncogenic fusion protein

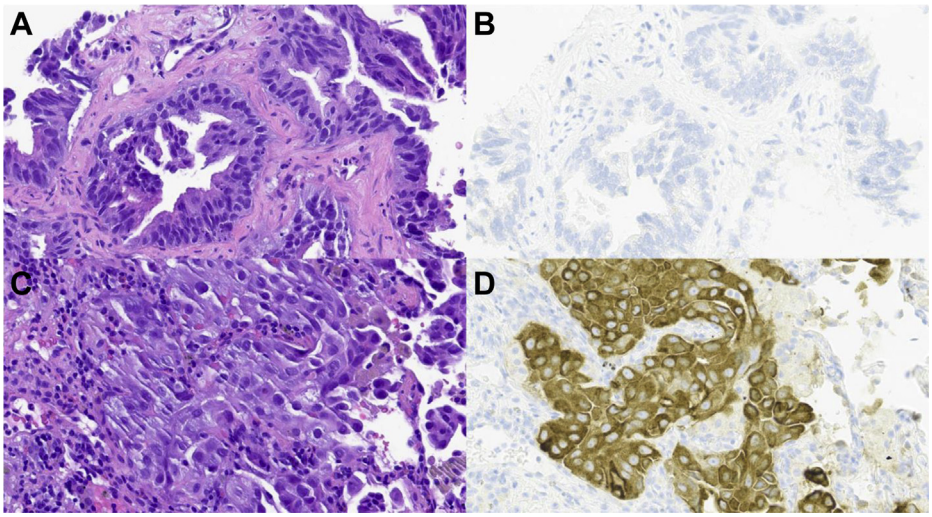

Figure 2. Examples of ROS1 SP384 IHC staining. (*A*) H&E stain of a case with no tumor cells staining in the corresponding (*B*) ROS1 SP384 IHC giving it a negative status. Next is (*C*) H&E stain of a case with moderate-to-strong staining in all the tumor cells in the corresponding (*D*) ROS1 SP384 IHC giving it a positive status. All digital images are at 400× magnification. H&E, hematoxylin and eosin; IHC, immunohistochemistry.

that is overexpressed, detectable by IHC, and will likely respond to ROS1 TKIs. On the other hand, the fusion genes with *PTPRK* and *TTC28* had little to no protein expression of ROS1 and were considered negative for ROS1 IHC on the basis of our analysis. Of note, patient 12 (*PTPRK-ROS1*) had 1% of tumor cells staining at 1+ (weak intensity), but it was not close to the cutoff examined by the two studies referenced previously and was considered negative for ROS1 IHC.[11,12,14] In addition, it is interesting to note that two of the three *ROS1* noncanonical fusions with negative ROS1 IHC staining had a later breakpoint (exon 35), though the n is small and no conclusion can be made from this finding. Overall, these findings highlight that a subset of *ROS1* fusions with noncanonical fusion partners are not detectable by routine ROS1 IHC testing. Notably, all three fusions (*PTPRK-ROS1* [2], *TTC28-ROS1*) retained an intact *ROS1* tyrosine kinase domain (exons 36–42); however, we hypothesize that the preserved kinase domain of these noncanonical *ROS1* fusions was not activated and is therefore not likely to respond to ROS1 TKIs. Although the mechanisms that allow for fusion-positive tumors to reveal a lack of ROS1 protein expression using the SP384 IHC assay remain unclear, further clinical studies that include therapy-specific clinical outcome results are warranted to determine the value of ROS1 TKIs in this subset of *ROS1* fusion–positive but ROS1 protein-negative cancers.

In addition, we examined ROS1 protein expression of a *ROS1-SDC4* case with a co-occurring known resistance mutation *ROS1* 6094 G>A (p.G2032R).[23] In this case, even though there was a ROS1 resistance mutation, the ROS1 oncogenic protein was still highly overexpressed. This is consistent with the proposed mechanism of action of the *ROS1* 6094 G>A mutation, in which the resistance to ROS1 kinase inhibition is caused by a steric interference with drug binding and not because of a down-regulation of protein expression.[24] This is important to highlight as one of the advantages of CGP which is the ability to not only detect targetable gene fusions, but also to detect concurrent TKI resistance mutations that might not otherwise be identified by other diagnostic methodologies (e.g., IHC).

We next sought to evaluate the ROS1 protein expression in a cohort of *ROS1* amplified (CN ranging from 7 to 20) tumors. Our findings revealed that one of 10 *ROS1* amplified cases found sufficient protein expression to be considered positive for ROS1 IHC on the basis of cutoff criteria. In our cohort of cases, we did not see an increase in protein expression with increasing *ROS1* CN changes. Importantly, there was one case, patient 18, that had ROS1 protein expression even though it was not considered positive on the basis of our cutoff. One point of consideration is that the cutoff criteria we used was based on *ROS1* fusions and not *ROS1* amplifications, so the clinical relevance of this case is less clear.[14] From this cohort of patients, we have some preliminary evidence that unlike *ERBB2* amplification and HER2 protein expression, *ROS1* gene amplification is not directly correlated to ROS1 protein expression. The clinical implications of ROS1 protein expression without *ROS1* canonical fusions needs to be further investigated in clinical studies that feature ROS1 TKI response data. In addition, we examined five cases with a variety of *ROS1* short-variant mutations and found no protein expression in any of those cases, highlighting that these

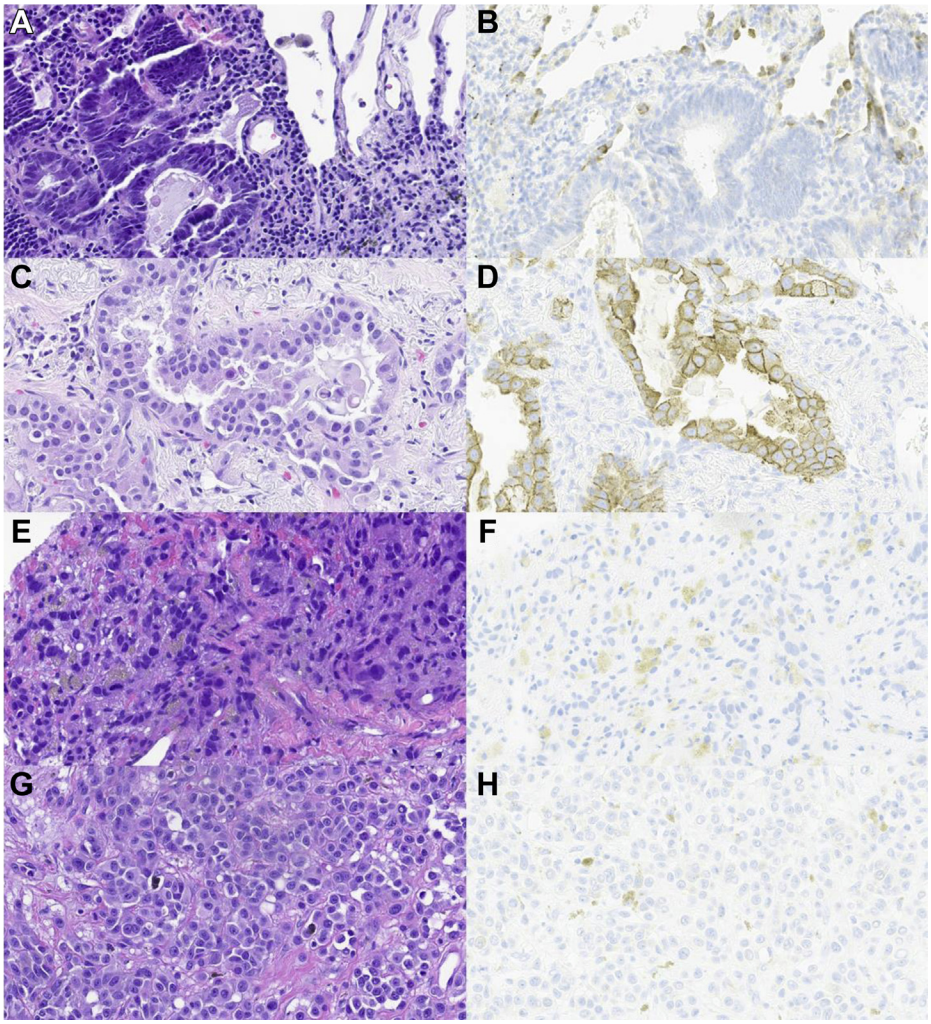

Figure 3. Examples of important staining patterns and artifacts with ROS1 SP384 IHC. (*A*) H&E stain of a case exemplifying moderate-to-strong staining in the reactive type II pneumocytes and no staining in the tumor cells in the corresponding (*B*) ROS1 SP384 IHC. Like other studies, we found that reactive type II pneumocytes can stain strongly for ROS1 SP384. As pathologists can readily distinguish tumor cell staining from type II pneumocyte staining, the presence of type II pneumocyte staining in lung cancer samples provides a reliable in situ control and can also serve as a run control for this assay. (*C*) H&E stain of a *ROS1-EZR* fusion case with moderate-to-strong membrane staining in the tumor cells in addition to cytoplasmic staining in the corresponding (*D*) ROS1 SP384 IHC. This is actual ROS1 IHC staining and occurs in a small proportion of *ROS1* fusion-positive cases. (*E*) H&E stain of a case with no tumor cells staining but some light brown staining of the hemosiderin in the corresponding (*F*) ROS1 SP384 IHC. This is artifactual staining and should not be confused with actual ROS1 SP384 staining. Finally, (*G*) H&E stain of a melanoma case with no staining in the tumor cells but with a yellow-brown staining of the melanin pigment in the corresponding (*H*) ROS1 SP384 IHC. This represents melanin pigmentation and should not be confused with actual ROS1 IHC staining. All digital images are at 400× magnification. H&E, hematoxylin and eosin; IHC, immunohistochemistry.

mutations do not likely lead to increased production of oncogenic proteins and will not likely be associated with clinical benefit from anti-ROS1 targeted therapies.

From this study, we found several interesting patterns of ROS1 SP384 staining. First, like other studies, we found that reactive type II pneumocytes can stain strongly for ROS1 SP384 (Fig. 3*A* and *B*). As pathologists can readily distinguish tumor cell staining from type II pneumocyte staining, the presence of type II pneumocyte staining in lung cancer samples provides a reliable in situ control and can also serve as a run control for this assay. In addition, similar to the ROSING study, we identified ROS1 membranous staining in 50% (two of four) of *ROS-EZR* fusions (Fig. 3*C* and *D*).[12] Finally, we identified hemosiderin artifact a melanin pigment artifact in two of the cases as illustrated in Figure 3*E* to *G*.

In conclusion, the identification of patients whose tumors are driven by *ROS1* alterations remains clinically important given available and effective targeted therapies. In this study of 32 *ROS1* altered tumors, the data

reveal that positive ROS1 IHC staining reliably identified tumors (11 of 11) harboring canonical *ROS1* fusions; however, only 40% (two of five) noncanonical *ROS1* fusions revealed positive IHC staining. In contrast, ROS1 IHC was positive in one tumor revealing *ROS1* gene amplification. Taken together, these findings suggest that if ROS1 IHC was used as a screening tool for targetable *ROS1* fusions, a subset of fusion-negative tumors will reveal positive IHC staining, highlighting the value of reflexing to genomic profiling to confirm the presence of a fusion-driver before the initiation of anti-ROS1 therapy. In addition, the ability of CGP to detect *ROS1* resistance mutations will be important for clinical decision making. Furthermore, we found that a subset of tumors harboring driver *ROS1* fusions was negative for ROS1 protein expression by IHC. Our hypothesis is that these IHC–negative but fusion-positive tumors have noncanonical *ROS1* fusions that do not activate the kinase domain of ROS1 and are not likely to respond to ROS1 TKIs, although this needs to be further validated by clinical studies.

Supplementary Data

Note: To access the supplementary material accompanying this article, visit the online version of the *JTO Clinical and Research Reports* at www.jtocrr.org and at https://doi.org/10.1016/j.jtocrr.2020.100100.

References

1. Nagarajan L, Louie E, Tsujimoto Y, Balduzzi PC, Huebner K, Croce CM. The human c-ros gene (ROS) is located at chromosome region 6q16–6q22. *Proc Natl Acad Sci U S A*. 1986;83:6568–6572.
2. Davies KD, Doebele RC. Molecular pathways: ROS1 fusion proteins in cancer. *Clin Cancer Res*. 2013;19:4040–4045.
3. Birchmeier C, Sharma S, Wigler M. Expression and rearrangement of the ROS1 gene in human glioblastoma cells. *Proc Natl Acad Sci U S A*. 1987;84:9270–9274.
4. Lin JJ, Shaw AT. Recent advances in targeting ROS1 in lung cancer. *J Thorac Oncol*. 2017;12:1611–1625.
5. Food and Drug Administration. FDA expands use of xalkori to treat rare form of advanced non-small cell lung cancer. https://www.fda.gov/news-events/press-announcements/fda-expands-use-xalkori-treat-rare-form-advanced-non-small-cell-lung-cancer. Accessed January 16, 2020.
6. Food and Drug Administration. FDA approves entrectinib for NTRK solid tumors and ROS-1 NSCLC. https://www.fda.gov/drugs/resources-information-approved-drugs/fda-approves-entrectinib-ntrk-solid-tumors-and-ros-1-nsclc. Accessed January 20, 2020.
7. Shaw AT, Solomon BJ. Crizotinib in ROS1-rearranged non-small-cell lung cancer. *N Engl J Med*. 2015;372:683–684.
8. Drilon A, Siena S, Dziadziuszko R, et al. Entrectinib in ROS1 fusion-positive non-small-cell lung cancer: integrated analysis of three phase 1-2 trials [published correction appears in *Lancet Oncol*. 2020;21:e70] [published correction appears in *Lancet Oncol*. 2020;21:e341]. *Lancet Oncol*. 2020;21:261–270.
9. Lindeman NI, Cagle PT, Aisner DL, et al. Updated molecular testing guideline for the selection of lung cancer patients for treatment with targeted tyrosine kinase inhibitors: guideline from the College of American Pathologists, the International Association for the Study of Lung Cancer, and the Association for Molecular Pathology. *J Thorac Oncol*. 2018;13:323–358.
10. National Comprehensive Cancer Network. NCCN clinical practice guidelines in oncology (NCCN guidelines): non-small cell lung cancer, version 5.2019. https://www2.tri-kobe.org/nccn/guideline/lung/english/non_small.pdf. Accessed January 20, 2020.
11. Hofman V, Rouquette I, Long-Mira E, et al. Multicenter evaluation of a novel ROS1 immunohistochemistry assay (SP384) for detection of ROS1 rearrangements in a large cohort of lung adenocarcinoma patients. *J Thorac Oncol*. 2019;14:1204–1212.
12. Conde E, Hernandez S, Martinez R, et al. Assessment of a new ROS1 immunohistochemistry clone (SP384) for the identification of ROS1 rearrangements in patients with non-small cell lung carcinoma: the ROSING study. *J Thorac Oncol*. 2019;14:2120–2132.
13. Nong L, Zhang Z, Xiong Y, et al. Comparison of next-generation sequencing and immunohistochemistry analysis for targeted therapy-related genomic status in lung cancer patients. *J Thorac Dis*. 2019;11:4992–5003.
14. Huang RSP, Smith D, Le CH, et al. Correlation of ROS1 immunohistochemistry with ROS1 fusion status determined by fluorescence in situ hybridization. *Arch Pathol Lab Med*. 2020;144:735–741.
15. Uguen A, De Braekeleer M. ROS1 fusions in cancer: a review. *Future Oncol*. 2016;12:1911–1928.
16. Rozenblum AB, Ilouze M, Dudnik E, et al. Clinical impact of hybrid capture-based next-generation sequencing on changes in treatment decisions in lung cancer. *J Thorac Oncol*. 2017;12:258–268.
17. Pishvaian MJ, Garrido-Laguna I, Liu SV, Multani PS, Chow-Maneval E, Rolfo C. Entrectinib in TRK and ROS1 fusion-positive metastatic pancreatic cancer. *JCO Precis Oncol*. 2018;2:1–7.
18. Zhu VW, Upadhyay D, Schrock AB, Gowen K, Ali SM, Ou SH. TPD52L1-ROS1, a new ROS1 fusion variant in lung adenosquamous cell carcinoma identified by comprehensive genomic profiling. *Lung Cancer*. 2016;97:48–50.
19. Donati M, Kastnerova L, Martinek P, et al. Spitz tumors with ROS1 fusions: a clinicopathological study of 6 cases, including FISH for chromosomal copy number alterations and mutation analysis using next-generation sequencing. *Am J Dermatopathol*. 2020;42:92–102.
20. Davare MA, Henderson JJ, Agarwal A, et al. Rare but recurrent ROS1 fusions resulting from chromosome 6q22 microdeletions are targetable oncogenes in glioma. *Clin Cancer Res*. 2018;24:6471–6482.
21. Newman AM, Bratman SV, Stehr H, et al. FACTERA: a practical method for the discovery of genomic rearrangements at breakpoint resolution. *Bioinformatics*. 2014;30:3390–3393.

22. Picco G, Chen ED, Alonso LG, et al. Functional linkage of gene fusions to cancer cell fitness assessed by pharmacological and CRISPR-Cas9 screening. *Nat Commun*. 2019;10:2198.
23. Guisier F, Piton N, Salaun M, Thiberville L. ROS1-rearranged NSCLC with secondary resistance mutation: case report and current perspectives. *Clin Lung Cancer*. 2019;20:e593–e596.
24. Roys A, Chang X, Liu Y, Xu X, Wu Y, Zuo D. Resistance mechanisms and potent-targeted therapies of ROS1-positive lung cancer. *Cancer Chemother Pharmacol*. 2019;84:679–688.
25. Frampton GM, Fichtenholtz A, Otto GA, et al. Development and validation of a clinical cancer genomic profiling test based on massively parallel DNA sequencing. *Nat Biotechnol*. 2013;31:1023–1031.
26. Connelly CF, Carrot-Zhang J, Stephens PJ, Frampton GM. Abstract 1227: somatic genome alterations in cancer as compared to inferred patient ancestry. *Cancer Res*. 2018;78(suppl 13):1227.
27. Carrot-Zhang J, Chambwe N, Damrauer JS, et al. Comprehensive analysis of genetic ancestry and its molecular correlates in cancer. *Cancer Cell*. 2020;37:639–654.e6.
28. VENTANA ROS1 (SP384) Rabbit monoclonal primary antibody [package insert], Toledo, OH: VM Systems; 2019.